ELSEVIER

Journal of Molecular Catalysis A: Chemical 187 (2002) 247–257

JOURNAL OF MOLECULAR CATALYSIS A: CHEMICAL

www.elsevier.com/locate/molcata

Molybdenum oxide based partial oxidation catalyst 4. TEM identification of a new oxygen-reduced phase formed during acrolein partial oxidation under reducing conditions

Y. Uchida [a,*], G. Mestl [b,1], O. Ovsitser [a], J. Jäger [a], A. Blume [a], R. Schlögl [a]

[a] *Department of Inorganic Chemistry, Fritz Haber Institute of the MPG, Faradayweg 4-6, 14195 Berlin, Germany*
[b] *Nanoscape AG, Frankfurter Ring 193a, 80807 Munich, Germany*

Received 13 March 2002; accepted 30 April 2002

Abstract

A new Mo-based structure was detected by high resolution transmission electron microscopy (HRTEM) and electron diffraction techniques in a molybdenum based mixed oxide catalyst after operation in the partial oxidation of acrolein at temperatures between 533 and 573 K for 9 h. This new crystalline phase has an orthorhombic crystal system. The structure has presumably a space group of *Pban*, but *Pmmn* cannot be excluded. XRD analysis was further used to refine this new Mo_2O_5 structure. The lattice constants were estimated to be $a = 1217.5$, $b = 374.7$ and $c = 404.4$ pm, respectively. The elemental composition of the crystal was determined by the EDAX system attached to the electron microscope to be about $(Mo_{0.6}V_{0.3}W_{0.1})_2O_{5-x}$. This new structure is discussed in relation to earlier reports on a comparable composition and with respect to its possible role for partial oxidation catalysis.

Keywords: HRTEM; SAED; Multielement mixed metal oxide catalysts; Acrolein oxidation

1. Introduction

Molybdenum based mixed oxide catalysts are applied, for instance, in the industrial production of acrylic acid [1–9]. The main metallic elements are Mo, V and W in these mixed metal oxides. This catalyst system is rather unique in the sense that it reaches high selectivities to acrylic acid of above 90% at simultaneously high acrolein conversions of also above 90%. Moreover, the high activity and selectivity of these catalysts remains constant for long time of operation in the industrial process. Accordingly, a detailed study of the structural details of such mixed oxide catalysts is of high interest for academia and industry when structure–activity relations are attempted which could explain the catalytic properties.

In previous articles, we reported on a broad physico-chemical and catalytic investigation of this type of mixed oxide materials [10–13]. It was shown that the actual working catalyst contained a $(MoVW)_5O_{14}$-type phase as its major component, which either could be preformed by high temperature anneal in inert gas [12], or which directly crystallized during the activation in the catalytic partial oxidation reaction of acrolein [13]. The catalytic performance developed with time on stream parallel to the crystallization of this $(MoVW)_5O_{14}$-type oxide [13]. Accordingly, this $(MoVW)_5O_{14}$ phase was suggested

* Corresponding author.
E-mail address: gerhard.mestl@nanoscape.de (G. Mestl).
[1] Co-corresponding author.

1381-1169/02/$ – see front matter © 2002 Published by Elsevier Science B.V.
PII: S1381-1169(02)00211-X

to play an outstanding role for the partial oxidation of acrolein.

In order to further deepen the understanding of this type of MoVW mixed oxide catalysts, the different phases formed in the mixed oxide catalyst during catalysis were further analyzed in detail by electron microscopy. In this study, a MoVW catalyst was investigated which was operated in the acrolein partial oxidation under varying feed compositions between 533 and 573 K for 9 h. Although HRTEM is not an in situ technique, it has to be noted that the crystalline phases, which are formed during the activation for many hours on stream, are stable and do not rapidly change their bulk structures when the reactor is quenched to room temperature and the samples are transferred to the microscope. Moreover, electron microscopy is an unique analytical tool for the structural characterization of extremely small crystals, which will escape detection by any other structural characterization method.

A new crystalline structure was detected in the MoVW mixed oxide catalyst after acrolein partial oxidation between 533 and 573 K for 9 h. All crystallized particles of this phase, found in the specimen, were smaller than 300 nm. This type of crystals is considered to be an oxygen reduced phase of the MoVW mixed oxide. The crystal structure was estimated from the space group determined from the obtained configuration of the electron diffraction spots.

2. Experimental

2.1. Preparation of specimens

Aqueous solutions of ammonium heptamolybdate (AHM), ammonium metavanadate (AMV) and ammonium metatungstate (AMT) were mixed in the respective transition metal concentrations in order to obtain the composition of 64% Mo, 27% V, and 9% W total metal content, respectively. This solution was then dried by evaporation. Water and ammonia was subsequently desorbed by heating the mixture to 673 K in inert gas. This solid nanocrystalline precursor is the starting material for the following structural and catalytic investigations [10–12].

The catalyst activation in the acrolein oxidation was carried out in a quartz tubular flow reactor (i.d. 4 mm) at 533–573 K for 9 h. The gas mixture was varied between 4 and 5 mol% acrolein, 7 and 8 mol% oxygen, and 20 mol% water, with the balance helium.

The specimen for electron microscopy was prepared by the usual powder microscopy technique. A small amount of the thermally activated oxide powder was ground in a mortar and dispersed in a neutral organic solvent, such as *n*-pentane, by ultrasonic. A small droplet of this dispersion was placed onto a copper specimen grid covered by a thin carbon micro-grid. The specimen was dried in air prior to the electron microscopic investigations.

2.2. Structural analysis

The electron microscopic investigations were mainly performed with a Philips CM 200 FEG and a CM 200 LaB_6 with double tilting specimen stages. The energy dispersive X-ray analyser system (EDAX) is installed on both electron microscopes.

X-ray diffraction (XRD) measurements were done at room temperature on a STOE STADI-P focusing monochromatic transmission diffractometer equipped with a with Ge(1 1 1) monochromator and a position sensitive detector. Cu Kα radiation was used. The phase analysis was performed with the STOE Win XPOW software package (version 1.06; Stoe Darmstadt, Germany) and with PowderCell (V 2.3; Bundesanstalt für Materialforschung und -prüfung (BAM), Berlin, Germany).

3. Results

3.1. TEM and SEAD

As mentioned in 1. Introduction, the MoVW mixed oxide catalysts consist of different phases depending on activation and reaction conditions: an amorphous portion, a nanocrystalline portion, particles with an intermediate structure between a non-crystalline and a crystallized phase—one phase named “bundle structure”, the other “corona structure”—and finally well-crystallized particles [10–13]. The crystalline part of the catalyst mainly consisted of two types of crystals, the MoO_3-type and the Mo_5O_{14}-type, depending on the treatment temperature and atmosphere [10–13].

The MoO_3-type crystals in the mixed oxide specimen, which was thermally activated in inert gas

atmosphere, exhibited the regular MoO_3-type crystal structure, as proven by the configuration of the diffraction spots in the reciprocal space [12]. These MoO_3-type crystals contained relatively high concentrations of V and W. Therefore, the determined lattice constants were slightly different from that of pure MoO_3 [12].

In contrast to the crystal structures reported in the previous publications [10–13], some crystals detected in the mixed oxide specimen, which was operated in the acrolein oxidation under the above mentioned conditions, seemed to have a structure different from the regular MoO_3-type. Fig. 1 shows a low magnification electron micrograph. The electron micrograph was obtained with an objective aperture in order to enhance the contrast of the crystalline particles from the non-crystalline portion. Almost all crystalline particles in the specimen were embedded in larger non-crystalline regions. The arrows in Fig. 1 indicate the locations of two crystals, which have defined boundaries in the micrograph. The crystallized particles, indicated by the arrows, exhibited this new unusual structure. The energy dispersive X-ray spectrum (EDX), also shown in Fig. 1, was obtained from the crystallized particle indicated by the lower left arrow in the micrograph. Fortunately, a few crystalline particles of this new type were found isolated from the amorphous matrix. These isolated crystalline particles were used in this study for the determination of the crystal structure by electron microscopy.

A survey of the diffraction spot configurations in the reciprocal space was used to determine the crystal structure of these particles. Fig. 2 shows examples of diffraction patterns obtained during tilting series of one isolated single crystal on the thin carbon film. The three-dimensional reciprocal lattice was constructed as schematically shown in Fig. 3 from diffraction patterns of more than 20 different tilting series (other series not shown). In Fig. 3, the corrected indices of the reflection points in the reciprocal space are given after the determination of the crystal system. The crystal system was found to be orthorhombic. The dimensions of the unit cell were estimated from the electron diffraction patterns to be $a = 1203$ pm, $b = 370$ pm, and $c = 399$ pm. These values were confirmed to be very precise by the conventional selected area electron diffraction technique.

The different intensities of the reciprocal lattice points are not considered in Fig. 3. The different intensities of the diffraction spots can of course easily be recognized in the experimental diffraction patterns. However, these intensity differences can only be understood as a tendency of the respective diffraction strength and not as a quantitative measure. Generally, the intensities of the diffraction spots have to be determined for an exact crystal structure analysis. The exact intensity measurement in electron diffraction, however, is almost impossible with the exception of some special cases. The intensity of a diffraction spot in electron diffraction patterns depends on many different factors, such as the excitation error for the corresponding reflection, the intensity and area of the illuminated crystal, the convergence of the electron beam, the thickness of the illuminated crystal, and other diffraction conditions for other reflections, etc. [14]. All these factors are almost impossible to control by the usual selected area electron diffraction technique. Therefore, the experimental intensities of the reflections were not taken into account for the zeroth approximation of the crystal model.

However, when convergent beam electron diffraction (CBED) patterns can be obtained of a well-oriented crystal with reasonable contrast, these patterns can be very useful for structure analysis. A CBED pattern contains much more information on the crystal structure than an usual diffraction pattern. Such CBED patterns were recorded, but found to be not as useful as expected due to their very low contrast resulting from the too small crystal dimensions. Additionally, the difficulty of fine orientation adjustment of these small crystals led to low data quality. Therefore, the CBED patterns could not used for structure determination.

The chemical composition of this type of crystals was determined using the EDAX system. The measured quantitative values scatter from crystal to crystal, but the average of the different measurements gave mean metal concentrations of 60% Mo, 30% V, and 10% W, respectively. These average metal concentrations are close to the stoichiometry of the prepared aqueous starting solutions. From this composition and the crystal structure, this new type of mixed oxide crystals can roughly be described by the chemical formula $(Mo_{0.6}V_{0.3}W_{0.1})_2O_{5-x}$. The oxygen concentration in the crystals, however, cannot be measured with acceptable precision.

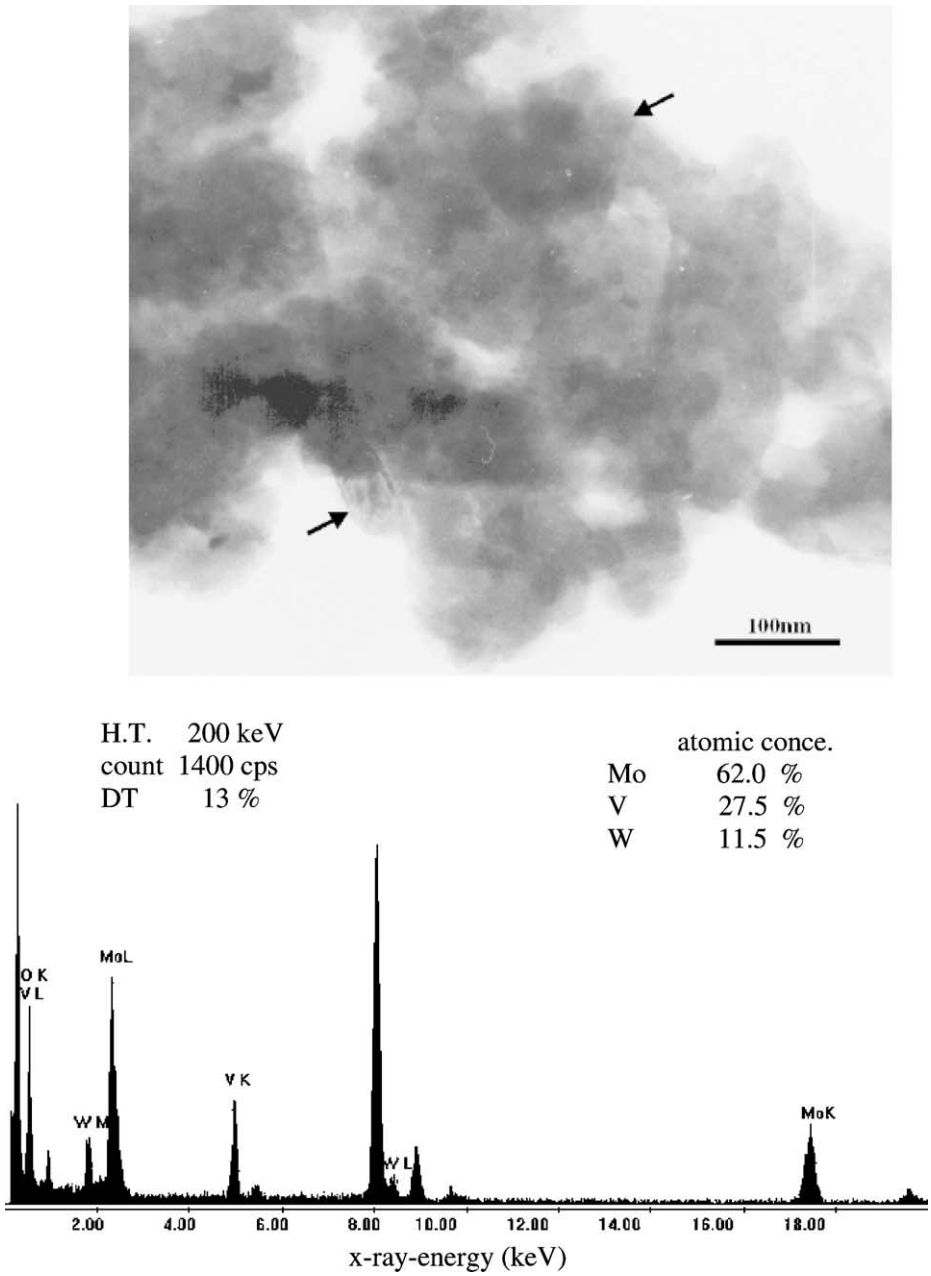

Fig. 1. Electron micrograph of the mixed oxide catalyst taken with objective aperture in order to enhance the contrast of crystallized particles. The sharp boundaries of crystallized particles are indicated by arrows. The EDX spectrum was taken from an isolated crystallized particle.

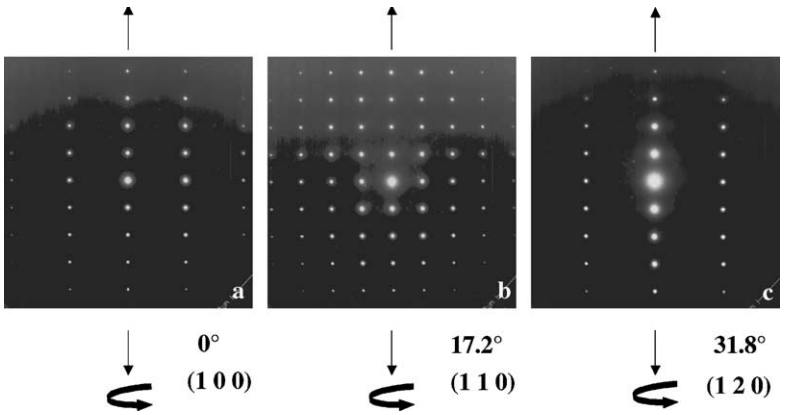

Fig. 2. Tilting series of diffraction patterns taken from an isolated small single crystal. The correct Miller indices are given for each pattern after crystallographic analysis.

3.2. X-ray diffraction

Because the precision of the unit cell dimensions as determined by electron diffraction is incomparable to that of a powder XRD analysis, XRD was additionally conducted on this sample. Fortunately, this catalyst, which was operated in the acrolein oxidation between 533 and 573 K for 9 h, contained mainly large portions of amorphous or nanocrystalline material, in which this new type of crystals were embedded, and only a very small amount of crystalline $(MoVW)_5O_{14}$-oxide.

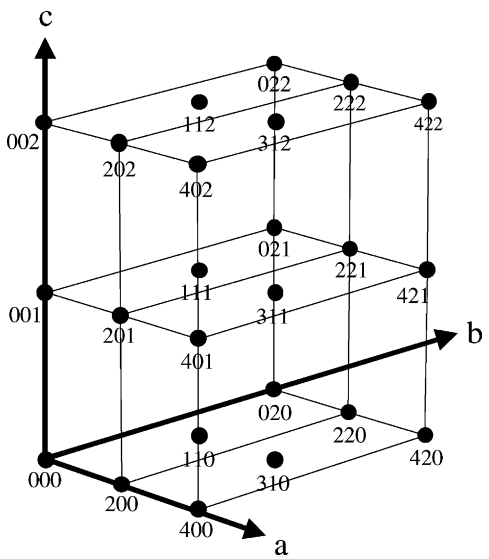

Fig. 3. The reciprocal lattice as obtained from the tilting series of electron diffraction patterns.

Fig. 4 shows the X-ray (diffractogram a) of this material. The high background can be recognized in this diffractogram, which is caused by the amorphous or nanocrystalline portion of the sample [10–13]. These nanocrystalline particles were also observed by electron microscopy and have been estimated to be smaller than 5 nm. Their crystal lattices obviously were not coherent enough to produce diffraction peaks in the XRD.

A further refinement of the lattice parameters as derived from the TEM data was carried out for this powder XRD data. The powder diffractogram (Fig. 4, diffractogram a) was composed of two independent phases, one of which was identified as the Mo_5O_{14}-type oxide. In order to reduce the influence of the Mo_5O_{14}-type oxide on the data evaluation, the diffractogram of the nanocrystalline reference Mo_5O_{14}-type oxide, as discussed in detail by Mestl et al. [11] and Dieterle et al. [12] (Fig. 4, diffractogram b) was subtracted from the experimental powder diffractogram (Fig. 4, diffractogram a). In addition, the diffraction pattern of the nanocrystalline reference was split into five 2Θ sections (Fig. 4, ranges 1–5). The XRD background of each $2T$ range was separately adapted to the measured diffractogram (Fig. 4, diffractogram a), combined, and subtracted from the experimental data. The diffraction pattern resulting from this data manipulation is also shown in Fig. 5 (diffractogram b).

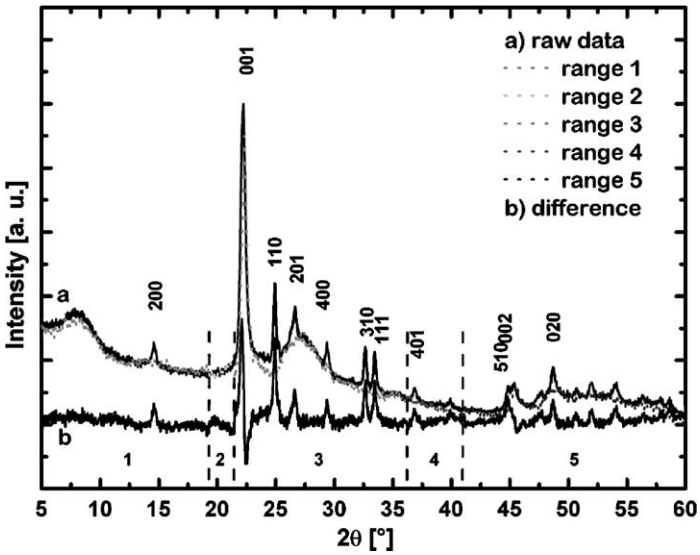

Fig. 4. Experimental XRD pattern of the $(MoVW)_2O_{5-x}$ containing catalyst (diffractogram a); XRD pattern after subtracting the background adapted from the reference XRD of nanocrystalline MoVW mixed oxide (diffractogram b) [1,2].

Fig. 5 once more displays the experimental XRD data (Fig. 5, diffractogram a) and the diffractogram of the nanocrystalline reference (diffractogram b) [10–12]. The diffractogram c of Fig. 5 was calculated on the basis of the oxide structure as postulated from the TEM results and further refined to the experimental XRD data. The refined lattice constants were determined to be $a = 1214(3)$ pm, $b = 373.9(0)$ pm,

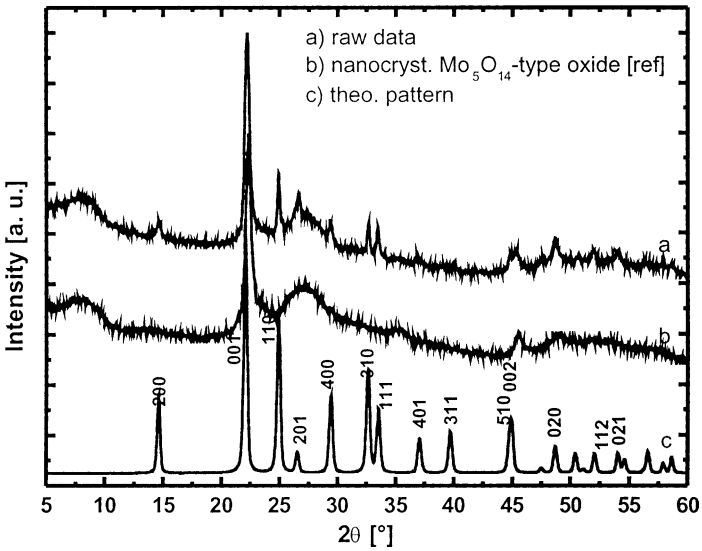

Fig. 5. XRD pattern of the MoVW mixed oxide operated in the acrolein oxidation (diffractogram a); reference XRD pattern of the nanocrystalline MoVW oxide prior to catalysis (diffractogram b) [1,2], XRD pattern simulated from the estimated space group and atomic positions (diffractogram c).

and $c = 403(0)$ pm. Only a few reflections, however, could be used for this refinement due to the highly symmetric space group. Accordingly, the accuracy of lattice constants of the (0 0 1) reflection of the $(MoVW)_2O_{5-x}$-type oxide and of the (0 0 1) reflection of the $(MoVW)_5O_{14}$-type oxide was not better than ±0.01 pm. Still, the obtained accuracy was an order of magnitude higher as compared to those of the lattice constants determined by the TEM-SAED analysis. The accuracy of the lattice parameter of the *c* axis is estimated to be lower with ±0.01 Å. This is due to the overlap of this reflection with the (0 0 1) reflection of the nanocrystalline Mo_5O_{14}-type oxide [10–12]. Hence, the XRD refinement of the lattice parameters markedly improved the accuracy of those obtained from TEM data.

3.3. Determination of the crystal structure

3.3.1. Determination of the space group

The determination procedure of the space group by electron diffraction is well known [15]. The extinction rules were determined from the electron diffraction patterns. These extinction rules are summarized in Table 1.

The unit cell structure as derived from the observed diffraction points is schematically shown in Fig. 3 without weighing the reflection points. Possible space groups could be selected for the investigated crystal from the extinction rules of diffraction spots (Table 1). The space group No. 50: *Pban* exactly satisfies the extinction rules of this crystal. In addition, all atoms in the unit cell have to be situated at special equivalent positions according to the condition for general indices *hkl* ($h + k = 2n$) [16]. A possible alternative space group is discussed below.

Table 1
Extinction rules for the newly detected oxygen-reduced MoVW phase

h k l	$h + k = 2n$
0 *k l*	$k = 2n$
h 0 *l*	$h = 2n$
h k 0	$h + k = 2I$
h 0 0	$h = 2n$
0 *k* 0	$k = 2n$
0 0 1	No condition

Due to the strong interaction between the electron wave and matter, it is often problematic to deduce the existence of an electron reflection from an experimental electron diffractogram. Forbidden diffraction spots often can be observed in the electron diffractogram due to double diffraction. Kinematically forbidden but dynamically allowed reflections can be distinguished from kinematically allowed reflections by CBED patterns [17]. But due to the mentioned weak contrast of the CBED, the crystal structure had to be determined without using the CBED pattern.

3.3.2. Determination of crystal structure

As mentioned above, the crystal system is orthorhombic and the crystal is suggested to be an oxygen-reduced phase of MoO_3, i.e. MoO_{3-x}. Hence, the dimensions of the unit cell are very similar to those of MoO_3, with the exception of the longest unit cell axis, *a*.

In the zeroth approximation, possible chemical compositions were considered for this unknown crystal in an attempt to determine the crystal structure. The unit cell volume was estimated to be 200 $Å^3$. It thus may contain four Mo atoms. The number of oxygen atoms cannot easily be estimated, but it is reasonable (vide supra) that the number of oxygen atoms in the unit cell is smaller than 12. Eleven oxygen atoms per unit cell are very unlikely due to the determined crystal symmetry. Therefore, a model crystal unit cell of space group No. 50 *Pban* was constructed with 10 oxygen atoms according to the following procedure: first, the special equivalent positions for the Mo atoms were considered. The *a*, *b* and *c* axes were appropriately chosen for the expected crystal symmetry. If the Mo atoms are placed in the unit cell at the 4*h* equivalent special positions (in Wyckoff's notation), only one parameter *x* remains to be determined. This parameter *x* could be estimated to lie between 0.14 and 0.16 from the intensity series of systematic 2*n* 0 0 reflections and from a consideration of possible Mo–Mo distances. Because the 2 0 0 and 4 0 0 diffraction spots have almost identical intensities, and because the 6 0 0 reflection is relatively strong too, the parameter *x* was chosen to be 0.15 for the zeroth approximation [18].

Other atomic positions were estimated from possible distances between oxygen and metal atoms. To this end, it has to be considered that the metal atoms in most transition metal oxides are positioned at the

Table 2
Atom positions for the suggested unit cell structure

Atom	Wyckoff	*x*	*y*	*z*
Mo, V, W	4h	0.15	0.0	0.5
O	4h	0.32	0.0	0.5
O	4j	0.15	0.0	0.0
O	4d	0.0	0.0	0.5

Space group No. *Pban*: $a = 121.75$ pm; $b = 37.47$ pm; $c = 40.44$ pm.

center of oxygen polyhedra, which are often so distorted that they can hardly be understood as octahedra. Accordingly, the 10 oxygen atoms were distributed at the special equivalent positions in order to coordinate the metal atoms by deformed oxygen octahedra. The suggested atomic positions for this model unit cell are summarized in Table 2. The atomic configurations in this model unit cell have higher symmetries than those of regular MoO_3, which will be discussed in the following section.

3.3.3. The alternative crystal model

The mixed-oxide catalyst was operated for 9 h between 533 and 573 K in a reducing atmosphere. Therefore, an alternative crystal model was speculatively considered of an oxygen-reduced phase of MoO_3. Fig. 6A schematically shows the atomic configuration of the MoO_3 unit cell [19]. MoO_3 has a layered structure with stacking in *b* direction. These layers are constructed from complex grids of metal and oxygen atoms. The layers weakly interact by oxygen–oxygen interactions (oxygen atoms *a*, *b* and *c*, *d*) as indicated in Fig. 6A. If the upper layer is shifted along these oxygen–oxygen interactions half a unit distance diagonally in the *ac* plane and additionally slid in the *b* direction, the oxygen atoms *a* and *b* will overlap. This operation is symmetry allowed, because the crystal has one-half diagonal glide structure in the *ac* plane at this position. An additional operation has to be applied between the oxygen atoms *c* and *d*. According to these operations, two oxygen atoms are removed from the MoO_3 unit cell. The resulting atomic configuration is schematically shown in Fig. 6B. The obtained unit cell dimension of 158.5 pm in *b* direction is smaller as compared to that of MoO_3. The crystal axes of the model in Fig. 6B are already changed to the appropriate axes as shown the

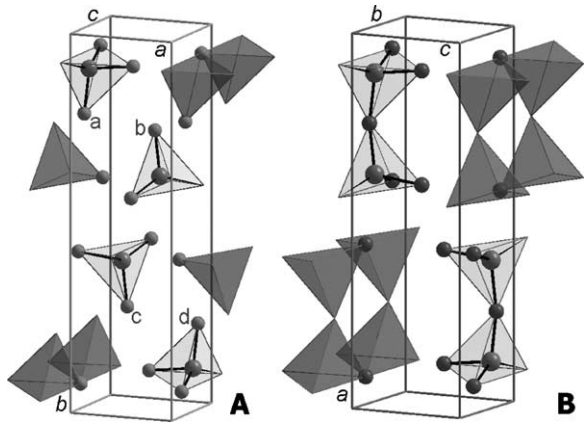

Fig. 6. (A) A schematic picture of atomic configuration in a unit cell of MoO_3. The oxygen–oxygen weak binding positions are indicated between *a* and *b*, and *c* and *d*; (B) a schematic picture of atomic configuration in a unit cell of the alternative crystal model. This crystal has been constructed through the two successive sliding operations at *a*–*b* and *c*–*d*, as described in the text.

figure. Accordingly, the unit cell dimensions should be $a = 1227.0$ pm, $b = 369.6$ pm and $c = 396.3$ pm, respectively. These values are very close to those of the detected crystal except the different choice of the crystal axes.

The crystal model deduced from regular MoO_3 has the space group No. 59 *Pmmn*. The atomic configuration of this alternative crystal model is listed in Table 3. The co-ordinate axes were changed to the system given in Table 2 for better comparison. Otherwise, this would be rather complicated due to the different space groups and the shifted origin. The comparison of both models reveals that the deviations in the positions of corresponding atoms is rather small. The largest deviation of about 35 pm was found for the metal atoms in *c* direction, the other deviations were much smaller.

Table 3
Atom positions of the alternative unit cell structure

Atom	Wyckoff	*x*	*y*	*z*
Mo, V, W	4f	0.1365	0.0	0.0867
O	4f	0.1533	0.0	0.5212
O	4f	0.3225	0.0	0.0006
O	2a	0.0	0.0	0.0373

Space group No. 59 *Pmmn*: $a = 121.75$ pm; $b = 37.47$ pm; $c = 40.44$ pm.

A crystal of this alternative model structure has to give a relatively strong 0 1 1 diffraction spot. However, such 0 1 1 spots could not be observed in the electron diffraction pattern as shown in Fig. 2a. Only very weak traces of a spot at the 0 1 1 position were detected in the diffraction patterns from a crystal which was irradiated in the electron beam for extended time periods (pattern not shown). Forbidden diffraction spots due to beam damage are often observed in the diffraction patterns of irradiated crystals. Therefore, the existence of a 0 1 1 reflection cannot unambiguously be deduced from the electron diffraction pattern. Hence, the alternative symmetry *Pmmn* can neither be confirmed nor excluded. Indeed the deviations of the atomic positions from those in the space group *Pban* are very small.

4. Discussion

The small crystals found in the molybdenum based mixed oxide after operation in the catalytic acrolein oxidation at 533–573 K for 9 h in varying feed compositions have an estimated composition of M_2O_{5-x}. It is highly interesting that this oxygen-reduced phase, formed during catalysis, does not belong to the so called Magnéli-type sub-oxides.

V_2O_5 crystallizes in the space group No. 59 *Pmmn* [20]. But the atomic configuration in the V_2O_5 unit cell is different from that of our model crystal structure or the alternative modified MoO_3 crystal model. This can easily be recognized from the ratios between the two short lattice constants of these structures, i.e. the *a*/*c* ratio for MoO_3 and the *c*/*b* ratio for V_2O_5 and our crystal model. These ratios are 1.226 for V_2O_5, 1.072 for MoO_3, and 1.079 for our crystal model, respectively. Accordingly, a unit cell structure like that of V_2O_5 can be excluded for the new Mo_2O_5 phase.

Strictly speaking, the crystal structure was not exactly determined by this approach. But a possible crystal model could be proposed with a relatively simple atomic configuration. Such a crystal structure with the space group No. 50 *Pban* is not reported yet for Mo oxides. The most crucial reasoning for this space group arises from the lack of 0 1 0, 0 1 1, 0 1 2, etc. reflections. However, the intensities of the reflections from these small crystals could not be precisely enough measured in the electron diffraction experiments. Thus, the existence of these reflections, and consequently, another space group cannot unambiguously be excluded. Additionally, the atomic positions could not be determined with the necessary precision for a full structure analysis.

Almost all crystals formed in the mixed oxide catalyst during operation in the acrolein oxidation under the mentioned conditions were smaller than about 300 nm. The elemental composition of the crystalline particles was roughly estimated by EDX to be about $(Mo_{0.6}V_{0.3}W_{0.1})_2O_{5-x}$. Vanadium and tungsten seemed to be randomly distributed in the crystalline particles. Evidence for an ordered substructure of the different metal ions in the crystal was not found in the diffraction patterns as indicated by the absence of fine-structure in the diffraction spots.

The existence of a stable crystalline Mo_2O_5 phase of pure molybdenum oxide remains unclear. Oxygen-reduced molybdenum oxides have been reported [21]. ϵ-Molybdenum oxide, first reported by Kihlborg and Magnéli [21], exhibits an X-ray powder diffraction pattern very similar to the present X-ray diffractogram (Fig. 5). But the differences in the two data sets are far beyond the experimental error. It might be argued that these differences may arise from the relatively large amounts of vanadium and tungsten in the present mixed oxide. On the other hand, the e-molybdenum oxide alternatively could be another phase of the presented crystal model. Nevertheless, the data reported for this e-oxide are too poor to be compared with our data with reasonable precision.

Recently, a very similar structure was reported by Plyasova et al. [22] who investigated V-Mo catalysts with about the same composition but without the additional W promoter. The reported stoichiometry of this oxide structure of $V_{0.95}Mo_{0.97}O_5$ was very close to the that determined in the present study. This $V_{0.95}Mo_{0.97}O_5$ oxide had a reported triclinic crystal system, P1, with the following lattice parameters $a = 633.40$, $b = 404.63$, $c = 372.55$ pm, $\alpha = 90.0^\circ$, $\beta = 107.3^\circ$, and $\gamma = 90.5^\circ$ and one formula unit per unit cell [22]. These unit cell parameters and the reported atom coordinates also allow the simulation of the diffraction patterns observed in the present study. However, it is suggested that the structure determined in the present study is indeed different from the literature report. From the presented angle-dependent HRTEM/SAED experiments, the presence of $\beta = 107.3^\circ$ can definitely be excluded. All SAED experi-

ments only revealed the orthorhombic crystal system. A deviation from 90° as big as 107° certainly would have been detected in the present experiments. It is suggested, that either the difference in the actual V concentration of both materials or the additional W promoter in the present oxide is responsible for the altered crystal structure. Alternatively, it might be suggested that the presence of twins in the sample of Plyasova et al. [22] might have led to their interpretation of the obtained XRD pattern. It was proposed that the triclinic $V_{0.05}Mo_{0.95}O_5$ oxide is highly active in the acrolein oxidation [23–26]. Definite statements about the intrinsic catalytic activity of this type of oxide in the acrolein oxidation cannot be drawn from the present study, because this structure was only present as a minority phase in the mixed phase oxide catalyst.

The new mixed $(MoVW)_2O_{5-x}$ crystals were less sensible to the electron beam irradiation as the mixed oxide crystals of the regular MoO_3-type. This may be explained by the different nature of atomic binding in both structures. The new mixed $(MoVW)_2O_{5-x}$ phase also seems to be more stable under electron irradiation than regular V_2O_5. This fact may also be explained by the different crystal structures. The higher stability of this $(MoVW)_2O_{5-x}$ phase could arise from its higher symmetric configuration as compared to MoO_3 or V_2O_5, which in turn may be caused by the reduced oxygen content in the crystal. Note that MoO_2 is also much more stable against electron irradiation and has a higher symmetry than MoO_3.

The sensitivity of oxide crystals to electron irradiation certainly depends on many different factors. However, the local symmetry around the metal atom seems to be very significant. Highly symmetric ReO_3 is very stable against electron irradiation. Nb_2O_5 and its sub-oxides are also stable under electron irradiation [27]. The crystal structures of these oxides are relatively complicated, but the local symmetry of each metal atom is high. On the other hand, MoO_3, V_2O_5 and their sub-oxides are relatively sensitive to electron irradiation. The peculiar, highly distorted configurations of oxygen atoms around the metal centers of these oxides are well known.

Powder XRD data were used to considerably increase the precision of the lattice constants. The exact atomic positions in the unit cell, however, could not be determined due to the contributions of the amorphous, nanocrystalline phase and the Mo_5O_{14}-type crystals in the specimen. In addition, there are further indications of a small amount of another, yet unknown crystalline phase in this mixed oxide catalyst complicating the analysis.

5. Conclusions

A new $(MoVW)_2O_{5-x}$ crystal structure is proposed for small crystals formed in the mixed oxide catalyst which was operated in the catalytic oxidation of acrolein between 533 and 573 K for 9 h under varying feed compositions. These small crystals are due to a molybdenum based vanadium and tungsten mixed oxide phase. The chemical composition of this crystal is estimated to be $(Mo_{0.6}V_{0.3}W_{0.1})_2O_{5-x}$.

The crystal belongs to an orthorhombic system and the space group is estimated to be *Pban*. The atomic configuration in the unit cell is also estimated. An alternative crystal model deduced from the regular MoO_3 structure is discussed for comparison.

This new $(MoVW)_2O$ oxide phase will further be investigated in the future in comparison to the active and selective $(MoVW)_5O_{14}$-type oxide in order to unravel its role in oxidation catalysis.

References

[1] A. Tenten, F.-G. Martin, H. Hibst H., L. Marosi, V. Kohl, BASF AG, European Patent 668104 B1 (1995).
[2] T. Kawajiri, S. Uchida, H. Hironaka, Nippon Shokubai Kagaku, European Patent 427508 A1 (1991).
[3] V. Novak, L. Sokol, J. Jelinek, CS 1207807 B (1981).
[4] N. Bertolini, S. Ferlazzo, Euteco Impianti S.p.A., US Patent 4289654 (1981).
[5] A.N. Kurtz, R.W. Cunningdam, A.W. Naumann, Union Carbide Co., US Patent 4111983 (1978).
[6] S. Breiter, M. Estenfelder, H.-G. Lintz, A. Tenten, H. Hibst, Appl. Catal. A 134 (1996) 81.
[7] K. Krauss, A. Drochner, M. Fehlings, J. Kunert, H. Vogel, J. Mol. Catal. A: Chem. 162 (2000) 413.
[8] L.B. Levy, P.B. Groot, J. Catal. 76 (1982) 385.
[9] P.B. Groot, L.B. Levy, J. Catal. 76 (1982) 393.
[10] H. Werner, O. Timpe, D. Herein, Y. Ushida, N. Pfänder, U. Wild, R. Schlögl, Catal. Lett. 44 (1997) 153–163.
[11] G. Mestl, Ch. Linsmeier, R. Gottschall, M. Dieterle, J. Find, D. Herein, J. Jäger, Y. Uchida, R. Schlögl, J. Mol. Catal. A 162 (2000) 455–484.
[12] M. Dieterle, G. Mestl, J. Jäger, Y. Uchida, H. Hibst, R. Schlögl, J. Mol. Catal. A 174 (2001) 169–185.

[13] O. Ovsitser, Y. Uchida, G. Mestl, G. Weinberg, A. Blume, M. Dieterle, H. Hibst, R. Schlögl, J. Mol. Catal. A, submitted for publication.
[14] D.B. Willams, C.B. Carter, Transmission Electron Microscopy, Plenum Press, New York, 1996, p. 201.
[15] B.F. Baxton, J. Eades, J.W. Steeds, G.M. Rackam, Phil. Trans. R. Soc. London 281 (1976) 171.
[16] N.E.M. Henry, K. Lonsdale (Eds.), International Tables for X-ray Crystallography, Vol. I, Kynoch Press, London, 1951.
[17] J. Gjønnes, A.F. Moodie, Acta Cryst. 19 (1965) 65.
[18] M. Buerger, Crystal Structure Analysis, Wiley, New York, 1960, p. 302.
[19] L. Kihlborg, Ark. Kemi. 21 (1963) 357.
[20] R. Enialbert, J. Galy, Acta Crystallogr. C42 (1986) 1469.
[21] L. Kihlborg, A. Magnéli, Acta Chem. Scand. 9 (1953) 471.
[22] M.L. Plyasova, L.P. Solov'eva, G.N. Kryukova, T.V. Andrushkevich, Kinet. Katal. 31 (1990) 1430–1434.
[23] T.V. Andrushkevich, L.M. Plyasova, T.G. Kznetsova, React. Kinet. Catal. Lett. 12 (1979) 463.
[24] T.G. Kuznetsova, G.K. Boreskov, T.V. Kuznetsova, React. Kinet. Catal. Lett. 12 (1979) 531.
[25] T.G. Kuznetsova, G.K. Boreskov, T.V. Andrushkevich, React. Kinet. Catal. Lett. 19 (1982) 405.
[26] T.V. Andrushkevich, T.G. Kuznetsova, Kinet. Katal. 27 (1986) 863.
[27] S. Iijima, private communication.